10

Optical properties of non-stoichiometric titanium oxides

© A.K. Gerasimova[1], V.A. Voronkovskii[1], D.A. Kalmykov[1], V.Sh. Aliev[1,3], V.A. Volodin[1,2], M.A. Demyanenko[1]

[1] Rzhanov Institute of Semiconductor Physics, Siberian Branch, Russian Academy of Sciences, Novosibirsk, Russia
[2] Novosibirsk State University, Novosibirsk, Russia
[3] Novosibirsk State Technical University, Novosibirsk, Russia

e-mail: aliev@isp.nsc.ru

Received October 22, 2024
Revised December 08, 2024
Accepted December 08, 2024

Optical properties of non-stoichiometric titanium oxides $TiO_{2-\delta}$ with different magnitude of deviation from stoichiometry δ have been investigated. The films were synthesized by ion-beam sputtering deposition method. The composition of the films was determined by X-ray photoelectron spectroscopy. The relationship between the optical parameters (n, k) of the films and their composition δ has been established. It was found that annealing of the films of the composition $\delta \sim 0.58 \pm 0.02$ at temperatures $350-600^{\circ}C$ leads to a significant increase in absorption in the THz regions of the spectrum due to the growth of micron-sized plate-shaped crystals in the films, according to the data of scanning electron microscopy.

Keywords: thin films, non-stoichiometric titanium oxides, X-ray photoelectron spectroscopy, spectral ellipsometry, optical losses.

DOI: 10.61011/EOS.2025.01.60567.7201-24

Introduction

Oxide films of transition metals have been widely used in microelectronics and continuously studied [1–3]. Optical properties of thin films of titanium dioxide are fundamentally depending on their synthesis method and further treatment [4–7]. This is explained by a structural diversity of titanium oxides resulting also in the diversity of their optical properties. The interest in non-stoichiometric titanium oxide films arose due to the fact that their partial or complete crystallization may result in the formation of crystalline phases with high electrical conductivity compared to the super-oxide TiO_2 [8]. As a result of crystallization, amorphous films $TiO_{2-\delta}$ $(\delta < 2)$ turn into a composite material: clusters with metallic conductivity enclosed in a dielectric matrix. Such a material has a high absorption coefficient and a high temperature coefficient of resistance, which is determined by the effective band gap of the dielectric matrix [9]. Despite the fact that titanium oxide films have long been practically used as heat-sensitive layers and there are some papers [10] describing the synthesis of such layers, no data on the relationship of parameter of deviation from stoichiometry δ with its optical properties was found in any publications. The purpose of this study was to investigate the effect of parameter δ on the optical properties of both, homogeneous and composite non-stoichiometric titanium oxide films in a wide spectral range from optical to terahertz. Composite films in this study were formed by thermal annealing of homogeneous films of non-stoichiometric composition. The study is of practical interest in terms of fabrication of heat-sensitive layers of microbolometers' arrays.

Film synthesis

The ion beam sputtering-deposition (IBSD) method was used to synthesize thin amorphous films of non-stoichiometric titanium oxides $TiO_{2-\delta}$ with precision composition control $(\delta = 0.02-1.18)$. The method is described in detail in paper [11]. The residual pressure in the vacuum chamber before the films sputtering was 10^{-4} Pa. A metallic target of specific purity titanium (Ti ¿ 99.92%) was used for sputtering. The target was sputtered with ions of Ar^+ with an energy of 1200 eV. The ion current density per target was kept constant and was 1.0 mA/cm^2. To obtain the oxides, high purity oxygen was supplied to the chamber $(O_2 > 99.999\%)$. Different values of the parameter δ were set by varying the oxygen supply. The partial pressure of oxygen in the growth domain ranged from $0.6 \cdot 10^{-3}$ to 10^{-2} Pa. The following wafers were used as substrates: Si(100) KEF-4.5 wafers (for ellipsometry) and double-side polished float-zone Si(100) wafers (for measurement of optical properties in the infrared (IR) spectrum) and Ge(wafers for terahertz (THz) spectrum). The temperature of the substrates during growth was no higher than70°C. The deposition rate, as well as the film thickness, were controlled by a quartz microbalance (Maxtek, Inc.). The growth rate according to the quartz sensor depended on

partial pressure of oxygen and was ~ 0.08 nm/s. According to ellipsometry the typical film thickness was about 50 nm. The films were annealed in an optical warm-up furnace at temperatures from the room temperature to 600°C in the pure argon environment with an addition of 2% vol.oxygen. The heating (cooling) rate was about 10°C/min. After heating to a preset temperature, the sample was kept at this temperature from 15 to 180 °min, and then cooled.

Research methods

The composition of the grown films was determined by X-ray photoelectron spectroscopy (XPS) on spectrometer SPECS UHV-Analysis-System with a spherical energy analyzer PHOIBOS 150 and a radiation source Al K_α ($E = 1486.74$ eV). The scale of the energy detector was calibrated on peaks Au $4f_{7/2}$ ($BE = 84.00 \pm 0.05$ eV) and Cu $2p_{3/2}$ ($BE = 932.66 \pm 0.05$ eV). To account for charging of the film surface, XPS spectra were aligned to the position of the carbon peak C 1*s* at 285.0 eV. Expansion of XPS experimental spectra in the energies region Ti 2*p* and O 1*s* was performed by Gaussian functions after background subtraction as per Shirley method. The ratio of atomic concentration of O to Ti was defined from the integral intensities of the photoelectronic lines O 1*s* and Ti 2*p* accounting for the corresponding coefficients of elements atomic sensitivity [12].

To find the optical constants of the film (refractive index n and absorption coefficient k) within the wavelengths (350−1100 nm) a spectral ellipsometer „ELLIPS-1891-SAG“ was used (Institute of Physical Problems SB RAS) [13]. The spectral resolution of the device was 2 nm, and the light beam incident angle on the sample was 70°. A four-zone measurement technique was used, followed by averaging over all four zones. The experimental spectra of ellipsometric angles Ψ and Δ were further compared with the calculated spectra obtained by solving the inverse ellipsometry problem. A single-layer optical model was used for ellipsometric calculations. The spectral dependences of ellipsometric angles in the entire spectral range for m number of points of the spectrum were adjusted by minimizing the error function σ:

$$\sigma^2 = \frac{1}{m}\sum_{i=1}^{m}\left[(\Delta_{\text{exp}} - \Delta_{\text{calc}})^2 + (\Psi_{\text{exp}} - \Psi_{\text{calc}})^2\right],$$

where Ψ_{exp}, Δ_{calc} and Ψ_{calc}, Δ_{calc} — experimental and calculated values of ellipsometric angles Ψ and Δ respectively, m — number of spectrum points. In IR range (2−20 μm) the films' optical parameters were measured using spectrophotometer Infralum FT-801, and in THz range using spectrometer Bruker VERTEX 80v.

The structural properties of $TiO_{2-\delta}$ films were studied using Raman scattering method on spectrometer T64000 (Horiba Jobin Yvon). The spectral resolution of RS spectrometer was not higher than 2 cm^{-1}. A solid-state fiber laser line with a wavelength of 514.5 nm was used for excitation. RS spectra were measured in backscattering geometry at room temperature. The polarization of the scattered light was not analyzed. The laser beam radiation power on a sample was 1 mW. In order to minimize the structures heating under laser beam, the sample was placed just below the focus, the spot size was about 8 μm. In addition to Raman scattering method, scanning electron microscopy (SEM) on a Hitachi SU8220 instrument was used to visualize clusters in films.

Table 1. Film samples $TiO_{2-\delta}$: P_{O2} — partial pressure of oxygen in chamber during growth, δ — deviation of chemical composition from stoichiometric data as obtained from XPS analysis

№	P_{O2} ($\times 10^{-3}$ Pa)	δ
T1	0.65	1.18
T2	1.22	0.58
T3	1.52	0.18
T4	1.77	0.11
T5	2.98	0.05
T6	9.23	0.02

Table 2. XPS data approximation parameters: BE (binding energy) — energy position of Gaussian line, FWHM — full width at half maximum

XPS-peak	Component	BE, eV	FWHM, eV
Ti $2p_{3/2}$	Ti^{4+}	458.75	1.09
	Ti^{3+}	458.30	1.09
	Ti^{2+}	457.10	1.09
	Ti^{1+}_{ads}	455.71	1.30
	Ti^{0}	454.20	1.30
O 1*s*	TiO_2	530.14	1.18
	Ti_2O_3	530.20	1.18
	TiO	531.80	1.18
	O_{ads}	531.10	2.63

Experimental findings and discussion

Composition of films

To compare the growth conditions and parameter δ, characterizing the composition deviation from the stoichiometric one, various titanium oxide films were grown (Table. 1). Further, these films were grown by XPS method.

To determine the parameter δ, the experimental peaks Ti 2*p* and O 1*s* were approximated by Gaussian lines, each of which corresponded to a certain degree of titanium oxidation. Due to spin-orbit splitting the peak Ti 2*p* is represented by a doublet of two Gaussian lines. The energy gap in the doublet was taken equal 5.8 eV, while the intensities ratio for Ti $2p_{1/2}$ and Ti $2p_{3/2}$ peaks — 1:2 [14].

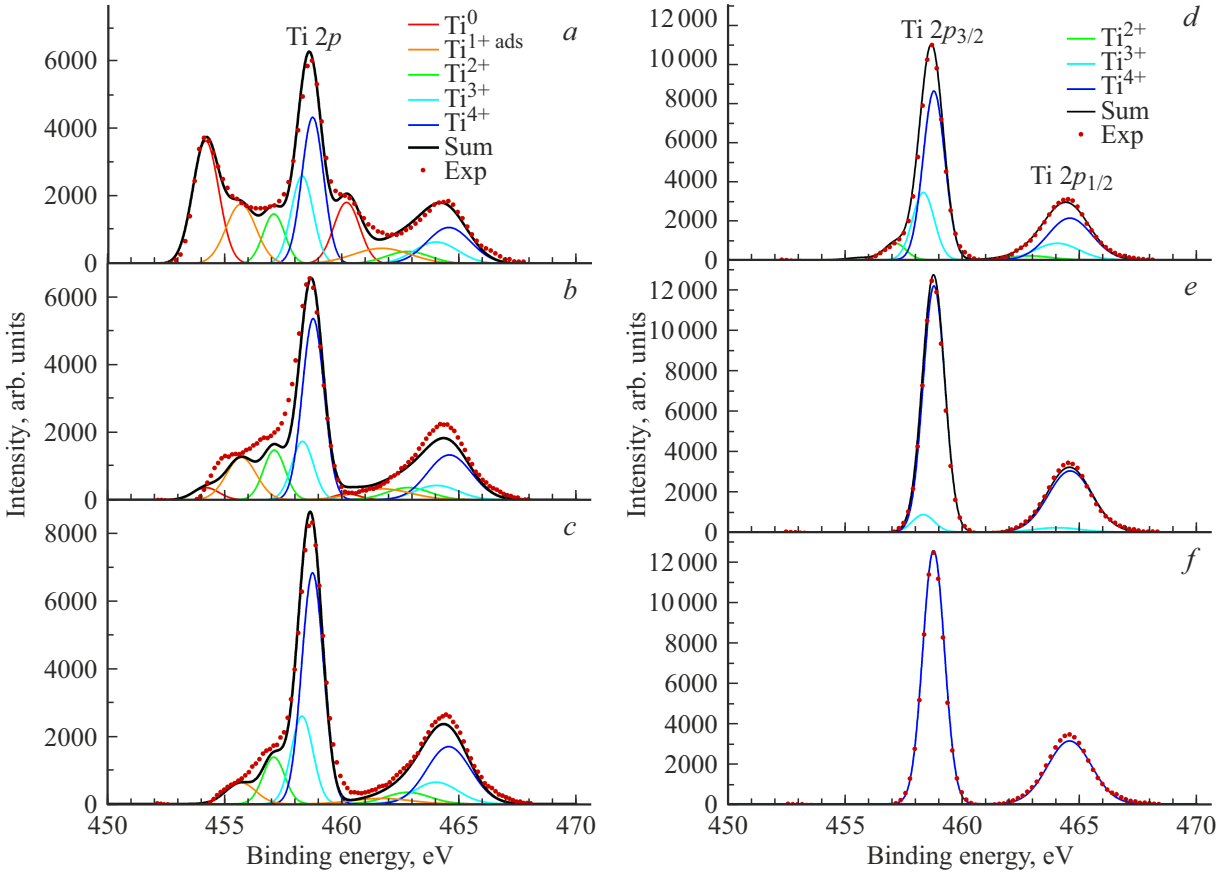

Figure 1. Experimental XPS-spectra (points) of $TiO_{2-\delta}$ films and their approximation within the energy levels range Ti 2*p*: *a* – T1, *b* — T2, *c* — T3, *d* — T4, *e* — T5, *f* — T6.

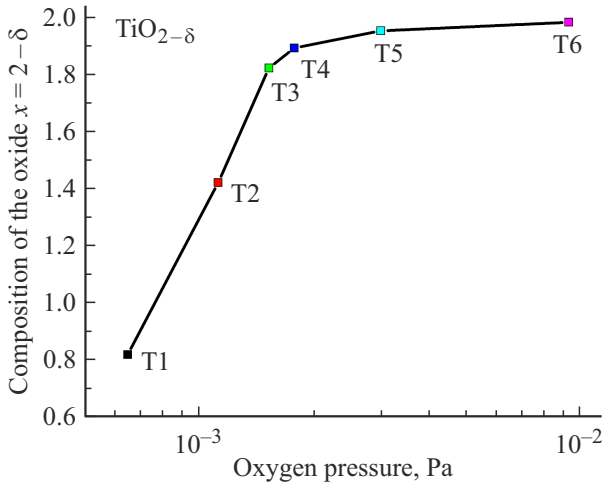

Figure 2. Stoichiometry coefficient $x = 2 - \delta$ versus partial pressure of oxygen in the growth chamber of TiO_x films.

The selection of the number of components was carried out in such a way as to approximate the experimental XPS-peaks with a minimum number of components, taking them in different proportions (Fig. 1). 4 components with the following oxidation states were used: Ti^{4+} in titanium oxide TiO_2, Ti^{3+} in titanium oxide Ti_2O_3, Ti^{2+} in titanium oxide TiO, component Ti^0, corresponding to metallic titanium. In addition, taking into account the non-stoichiometric composition and amorphous structure of the films, the peak Ti^{1+} was added. A similar decomposition into Gaussian lines was performed for experimental peaks of O 1*s*. The Gaussian lines parameters were selected with self-consistency for both peaks Ti $2p_{3/2}-2p_{1/2}$ and O 1*s* and for all samples. Parameters of Gaussian lines corresponding to the minimum deviation of the experimental points from the theoretical curves are presented in Table 2. The broadening of peaks Ti^0 and Ti^{1+} in comparison with other titanium peaks is probably due to oxygen adsorption on the samples surface. Broadening was also observed for component O_{ads} of the oxygen peak O 1*s*. This component of the oxygen peak, just as it was done in paper [15], was not taken into account when calculating the parameter δ. Selected parameters of Gaussian lines (Table 2) have good approximation of experimental results and are consistent with the known tabular XPS-data of TiO_2 [16]. The obtained dependence δ on oxygen partial pressure in the growth area (Fig. 2) made it possible to further determine the composition of films without XPS- measurements.

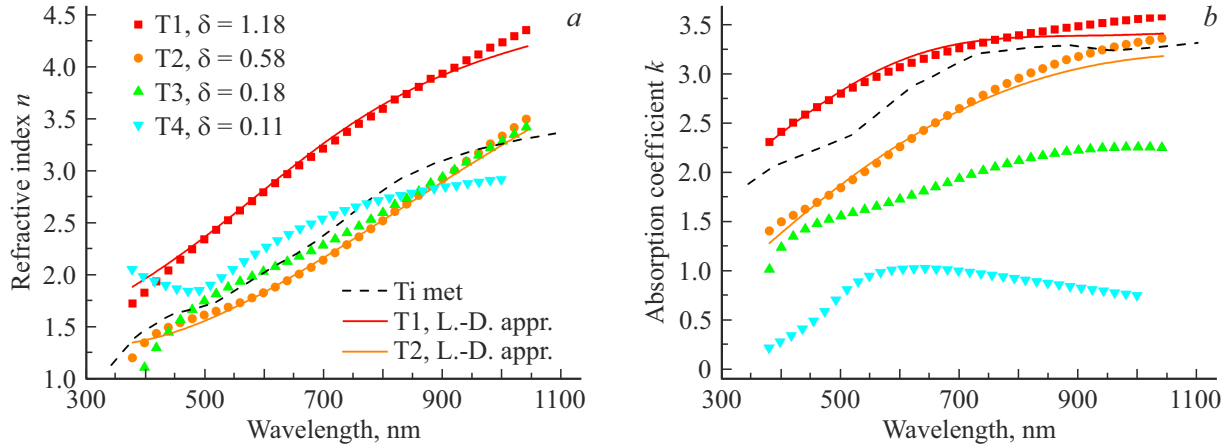

Figure 3. Experimentally obtained spectral dependences of refractive and absorption indices of films $TiO_{2-\delta}$ (dots) and their approximation (solid lines). Data for metallic titanium were taken from the database [17] and shown as a dashed line.

Table 3. Model parameters for approximating optical properties of metal films

№	δ	Lorentz-Drude model					
		e_∞, eV	E_{1D}, eV	E_{2D}, eV	A_i	E_i, eV	Γ_i
T1	1.18	2.0	19	15	9.5	1.7	1.1
T2	0.58	3.0	12	17	19.0	1.1	1.2

Optical properties in visible and near IR regions

The optical constants (n, k — respectively, the real and imaginary parts of the complex refractive index) of non-annealed films in visible and near-infrared spectral regions are shown in Figs. 3 and 4. T1 and T2 films are highly absorbent with anomalous dispersion, which is typical for metallic films. The optical constants of metallic titanium are presented for comparison [17]. Absorption coefficient k for metallic titanium is close to the absorption coefficient for T1 film, and absorption coefficient n — to T2-T4 films.

Optical constants of T1 and T2 films are well approximated via Lorentz-Drude oscillator model [18]:

$$\dot{\varepsilon}(\mathbf{E}) = \varepsilon_\infty - \frac{E_{1\rho}^2}{E^2 - jE_{2\rho}E} + \sum_{i=1}^{\theta} \frac{A_i E_i^2}{E_i^2 - E^2 + j\Gamma_i E_i E}, \quad (1)$$

where $\dot{\varepsilon}(E)$ — function of complex dielectric permittivity of photon energy, $E = hc/\lambda$ — photon energy, h — Planck constant, c — light velocity in vacuum, j — imaginary unit, ε_∞ — value of $\dot{\varepsilon}(E)$ at $E \to \infty$. Second term of expression (1) implies the contribution of the free charge-carriers, $E_{1\rho}$, $E_{2\rho}$ — constants. The third term describes the contribution of inter-band transitions as the excitation of damped harmonic oscillators: A_i, E_i and Γ_i — respectively, the force, energy and broadening function of i-th oscillator among θ taken into account. It turned out that for a satisfactory approximation of the experimental spectra, it

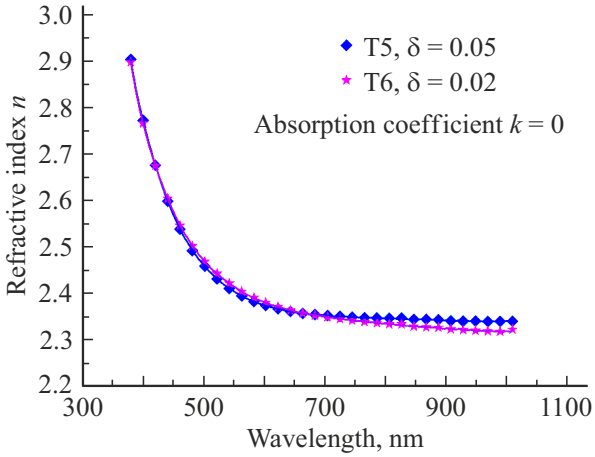

Figure 4. Spectral dependencies $n(\lambda)$ for $TiO_{2-\delta}$ films at $\delta < 0.05$ (dots) and their approximation via Cauchy model (solid lines).

was sufficient to use only one term in the sum describing the inter-band transitions ($\theta = 1$). The dispersion functions $n(\lambda)$ and $k(\lambda)$ for absorbing films were calculated by the ratio: $\dot{\varepsilon}(E) = \dot{N}(E)^2$, where $\dot{N}(E) = n(E) - jk(E)$ — complex refractive index. The data obtained are listed in Table 3.

For samples T5 and T6, the dispersion looked normal (refractive index n decreased with increasing wavelength, and the absorption coefficient $k = 0$). This dependence is well described using the polynomial Cauchy dispersion

Table 4. Model parameters for approximating optical properties of dielectric films

№	δ	Cauchy model		
		a	b	c
T5	0.05	2.30	$1.00 \cdot 10^4$	$130 \cdot 10^8$
T6	0.02	2.20	$8.33 \cdot 10^4$	$1.98 \cdot 10^{10}$

model, which is used to describe transparent dielectrics:

$$n(\lambda) = a + \frac{b}{\lambda^2} + \frac{c}{\lambda^4},$$

where a, b, c — Cauchy coefficients (Table 4).

Annealing of the films did not affect their optical properties at temperatures up to 300°C, which indicates a sufficiently high stability of non-stoichiometric films. Significant changes in optical constants (n, k) were observed only after annealing 600°C and only for films samples $\delta > 0.11$ (T2, T3) (Fig. 5). Optical constants of films samples with $\delta \leq 0.11$ (T4–T6) remained practically unchanged.

Optical spectra $n(\lambda)$ and $k(\lambda)$ for T3 and T4 films could be approximated neither by Cauchy model nor by Lorentz-Drude model (Fig. 3). By the nature of their optical spectra, they occupy a transition region between metallic and dielectric films. The T3 sample is closer to metallic in terms of properties and contains metal clusters, and T4 — to dielectric and does not contain metal clusters, which was confirmed by plasmon peaks in RS spectra.

RS spectra

When the deviation from stoichiometry was large enough the film of T1 sample ($\delta = 1.18$) turned out to be non-transparent for the excitation emission ($\lambda = 514.5$ nm) (Fig. 6, *a*). Therefore, the signal in RS spectrum from the silicon substrate was not observed. With lower δ and higher transparency of the film a peak appeared responsible for the long-wavelength optical phonon 520.6 cm^{-1} in silicon, as well as singularities related to the two-phonon scattering — two acoustic phonons (2TA, 300 cm^{-1}), optical and acoustic phonons (TO + TA, 650 cm^{-1}). In addition, in samples T2–T3, the RS spectra showed the presence of a wide peak, presumably corresponding to plasmons. In T4 sample the plasmon peak was not manifested clearly. Plasmonic peaks can be associated with the presence of crystal clusters with high conductivity in the films. A further decrease in the parameter δ (samples T5 and T6) led to the disappearance of plasmons. Annealing of films at temperature 330°C showed an increase in plasmon peaks in samples T2 and T3. The starting material for cluster growth in non-stoichiometric films are titanium atoms (or oxygen vacancies) that are excessive in comparison with the stoichiometric composition, which apparently have the ability to diffuse even at low temperatures (330°C). Probably, with a decrease in parameter δ , such Ti atoms (oxygen vacancies) begin to be lacking for cluster growth.

RS spectra showed that clusters are present in T2 and T3 films both, before and after annealing. It was unexpected that SEM method failed to visualize such clusters. It was probably because of insufficient resolution of SEM, which was bout 10 nm.

Structure according to SEM data

RS spectra have shown that clusters are present in samples with metallic spectral dependences of optical constants (Fig. 6). Therefore, the samples with $\delta > 0.11$ (T1–T3) were taken for structural studies. According to SEM data, the initial structure of the synthesized films was amorphous and remained so during annealing to temperatures of 300°C. Since it was found that significant differences in the optical spectra are observed during annealing at higher temperatures (Fig. 5), the samples were annealed at a temperature of 600°C for 15 min.

The crystal structure was most clearly manifested after annealing of T2 and T3 film samples (Fig. 7). SEM image shows the appearance of micron crystals in the films. Considering the thickness of initial films, which was 80 nm the crystals obviously have a lamellar shape.

Optical losses in IR and THz regions

The most interesting from practical standpoint are composite films, i.e. consisting of conductive clusters in a dielectric matrix [9]. These are $\delta > 0.11$ films. It should be noted that in these films, changes in optical properties are most pronounced during annealing: a multiple increase in the absorption coefficient was observed k (Fig. 5, *b*). To study optical losses in IR and terahertz regions of the spectrum, 300 nm thick films grown on double-side polished Si (FZ) substrates and Ge substrates were used. Optical losses (A) were found by formula $A = 1 - R - T$, where R and T — reflectance and transmittance coefficients, respectively.

Fig. 8, *a* illustrates the spectra of optical losses for the samples of films grown with $\delta = 0.18, 0.58$ for IR spectrum region (*b*) — with $\delta = 0.58$ for THz spectrum region. The spectra are presented after smoothing the interference peaks. It can be seen that annealing of films increases optical losses in both, IR and terahertz ranges of electromagnetic radiation. Obviously, the increase in optical losses is a consequence of the formation of a composite material due to the crystallization of films. In the terahertz region of the spectrum, the effect of annealing on optical losses is more significant, probably due to the formation of lamellar clusters with sizes reaching several microns.

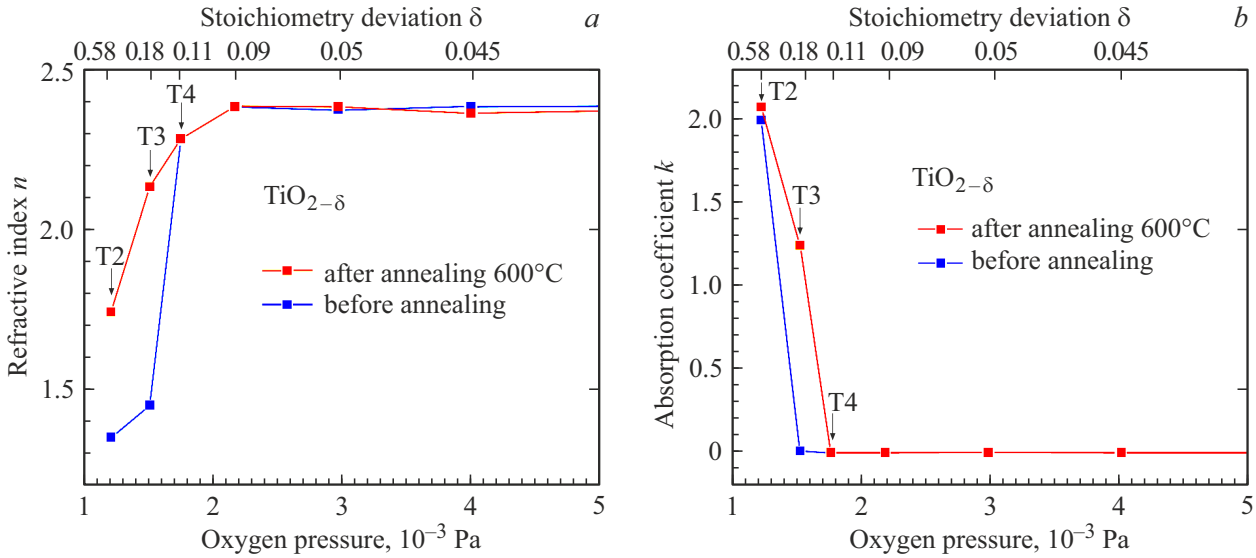

Figure 5. Dependencies (a) of refractive index n and (b) of absorption coefficient k according to ellipsometry data at light wavelength of $\lambda = 532.8$ nm for $TiO_{2-\delta}$ films on the partial pressure of oxygen and on parameter δ.

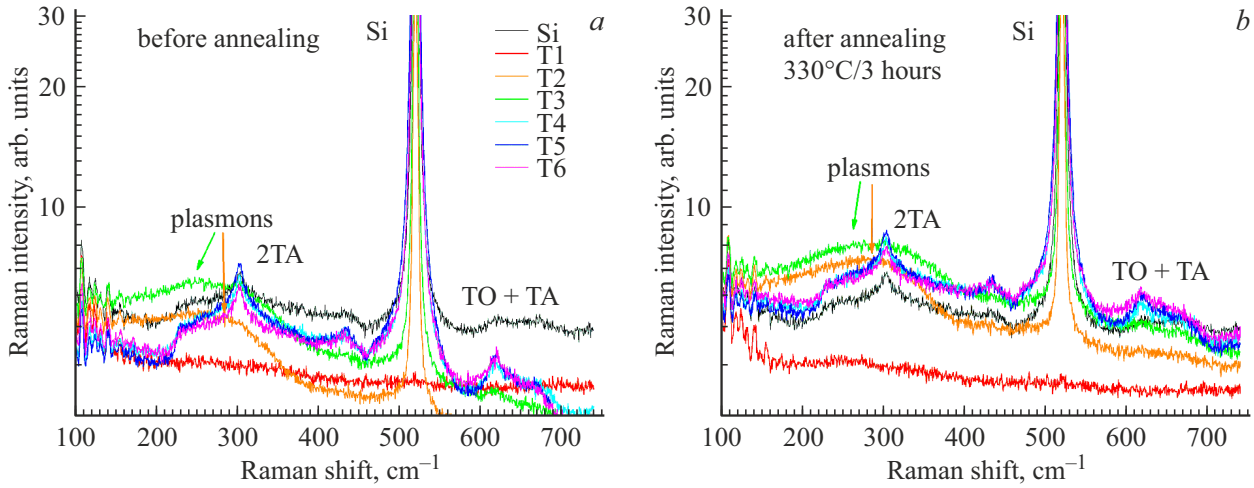

Figure 6. RS spectra before annealing (a) and after annealing (b) at 330°C during 3 h.

Conclusion

A laboratory technology has been developed for the synthesis of thin amorphous films of non-stoichiometric titanium oxides $TiO_{2-\delta}$ with precision composition control over a wide range ($\delta = 0.02-1.18$). An relationship between parameter δ and optical constants $n(\lambda)$ and $k(\lambda)$ in visible and near-infrared wavelength bands ($\lambda = 0.35-1.0\,\mu$m) was found. Films with a deviation from the stoichiometry $\delta > 0.18$ exhibit metallic properties, and optical constants are well described in the framework of Lorentz-Drude model. Films with a deviation of $\delta < 0.05$ behave like dielectric films, and the optical constants are described by Cauchy model. Annealing of films at temperature 600°C in argon atmosphere with a 2% volume addition of oxygen leads to a significant change in the optical properties of metal films, but does not affect the dielectric films. In IR and THz bands, annealing of films with $\delta > 0.18$ increases optical losses in films, which is probably explained by higher size of conducting clusters in the dielectric matrix. Films with $\delta = 0.11-0.58$ are of great interest for creating heat-sensitive layers of microbolometers' arrays.

Acknowledgments

The authors express their thanks to the employees of Institute of Physical Problems SB RAS A.S. Yaroshevich for assistance in defining optical losses in THz region of spectrum, Yu.A. Zhivodkov for analysis by SEM-method (Center of Collective Use „Nanostructures" Institute of Physical Problems SB RAS) and V.A. Golyashov for measurement of XPS-spectra.

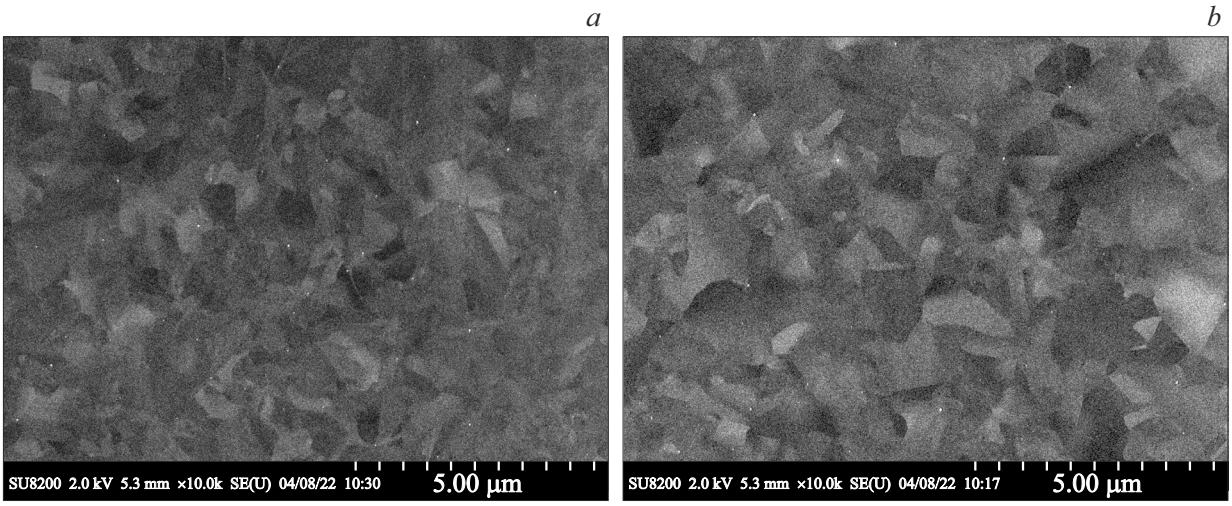

Figure 7. SEM-images of $TiO_{2-\delta}$ films surface after annealing at 600°C with deviation from stoichiometry $\delta = 0.58$ (*a*), 0.18 (*b*).

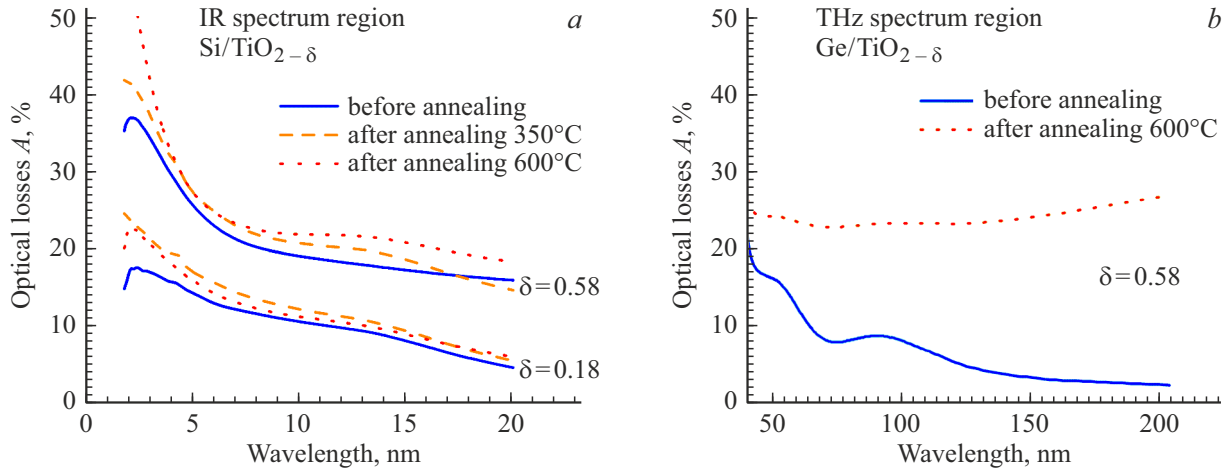

Figure 8. Optical losses (*A*) of films $TiO_{2-\delta}$: *a* — on Si substrate (FZ, substrate thickness of 380 μm) in IR spectrum; *b* — on Ge substrate (substrate thickness of 1 mm) in THz region of spectrum.

Funding

This study was supported by a grant from the Russian Science Foundation (project No. 24-29-00344).

Conflict of interest

The authors declare that they have no conflict of interest.

References

[1] V.N. Kruchinin, V.Sh. Aliev, A.K. Gerasimova, V.A. Gritsenko. Opt. i spektr., **121** (2), 260–265 (2016) (in Russian). DOI: 10.7868/S0030403416080092

[2] V.N. Kruchinin, V.A. Volodin, T.V. Perevalov, A.K. Gerasimova, V.Sh. Aliev, V.A. Gritsenko. Opt. i spektr., **124** (6), 777–782 (2018) (in Russian). DOI: 10.21883/OS.2018.06.46080.39-18

[3] V.N. Kruchinin, T.V. Perevalov, V.Sh. Aliev, R.M.Kh. Iskhakzai, E.V. Spesivtsev, V.A. Gritsenko, V.A. Pustovarov . Opt. and spektr., **128** (10), 1467–1472 (2020). DOI: 10.21883/OS.2020.10.50016.12-20

[4] Y. Ashok Kumar Reddy, Y.B. Shin, I.K. Kang, H.C. Lee, P. Sreedhara Reddy. Appl. Phys. Lett., **107** (2), 023503 (2015). DOI: 10.1063/1.4926604

[5] S.A. Gavrilov, A.A. Dronov, V.I. Shevyakov, A.N. Belov, E.A. Poltoratskiy. Rossiyskiye nanotekhnologii, **4** (3–4), 123–129 (2009) (in Russian).

[6] Y. Ju, Z. Wu, S. Li, X. Dong, Y. Jiang, J. Nanoelectron. Optoelectron., **7** (3), 317–321 (2012). DOI: 10.1166/jno.2012.1308

[7] A.A. Goncharov, A.N. Dobrovolsky, E.G. Kostin, I.S. Petrik, E.K. Frolova. ZhTF, **84** (6), 98–106 (2014) (in Russian). URL: https://journals.ioffe.ru/articles/viewPDF/ 27261

[8] H. Malik, S. Sarkar, S. Mohanty, K. Carlson. Sci. Rep., **10** (1), 8050 (2020). DOI: 10.1038/s41598-020-64918-0

[9] Y. Reddy, Y.B. Shin, I.K. Kang, H.C. Lee. J. Appl. Phys., **119** (4), 044504 (2016). DOI: 10.1063/1.4940957

[10] L. Li, Z. Wu, Y. Ju, C. Chen. Energy Procedia, **12**, 456–461 (2011). DOI: 10.1016/j.egypro.2011.10.061
[11] V.A. Shvets, V.Sh. Aliev, D.V. Gritsenko, S.S. Shaimeev, E.V. Fedosenko, S.V. Rykhlitski, V.V. Atuchin, V.A. Gritsenko, V.M. Tapilin, H. Wong. J. Non-Crystall. Sol., **354**, 3025–3033 (2008). DOI: 10.1016/j.jnoncrysol.2007.12.013
[12] J.H. Scofield. J. Electron Spectrosc. Rel. Phenomena, **8** (2), 129–137 (1976). DOI: 10.1016/0368-2048(76)80015-1
[13] S.V. Rykhlitsky, E.V. Spesivtsev, V.A. Shvets, V.Yu. Prokopiev. PTE **2, 161** (2012) (in Russian). DOI: 10.21883/OS.2019.11.48513.136-19
[14] J.F. Moudler, W.F. Stickle, P.E. Sobol, K.D. Bomben. *Handbook of X-ray photoelectron spectroscopy* (Perkin-Elmer, Eden Prairie, 1992).
[15] V.S. Aliev, A.K. Gerasimova, V.N. Kruchinin, V.A. Gritsenko, I.P. Prosvirin, I.A. Badmaeva. Mater. Res. Expr., **3** (8), 085008 (2016). DOI: 10.1088/2053-1591/3/8/085008
[16] *Fundamental XPS Data from Pure Elements, Pure Oxides, and Chemical Compounds*. URL: http://www.xpsdata.com/fundxps.pdf
[17] S. Adachi. *Optical Constants of Crystalline and Amorphous Semiconductors: Numerical Data and Graphical Information* (Springer Science + Business Media, 2013).
[18] W.S. Werner, K. Glantschnig, C. Ambrosch-Draxl. J. Phys. Chem. Ref. Data, **38** (4), 1013–1092 (2009). DOI: 10.1063/1.3243762

Translated by T.Zorina